A Novel Approach for Detection of Tubular Objects and Its Application to Medical Image Analysis

2 authors, including:

A Novel Approach for Detection of Tubular Objects and Its Application to Medical Image Analysis⋆

Christian Bauer and Horst Bischof

Institute for Computer Graphics and Vision, Graz University of Technology, Austria
{cbauer, bischof}@icg.tu-graz.ac.at

Abstract. We present a novel approach for detection of tubular objects in medical images. Conventional tube detection / lineness filters make use of local derivatives at multiple scales using a linear scale space; however, using a linear scale space may result in an undesired diffusion of nearby structures into one another and this leads to problems such as detection of two tangenting tubes as one single tube. To avoid this problem, we propose to replace the multi-scale computation of the gradient vectors by the Gradient Vector Flow, because it allows an edge-preserving diffusion of gradient information. Applying Frangi's vesselness measure to the resulting vector field allows detection of centerlines from tubular objects, independent of the tubes size and contrast. Results and comparisons to related methods on synthetic and clinical datasets show a high robustness to image noise and to disturbances outside the tubular objects.

1   Introduction

The detection and description of tubular structures, like blood vessels or airways is important for several medical image analysis tasks. The derived representations of the tubes, which are typically based on centerline descriptions, are used for visualization, interaction, initialization of segmentations, registration tasks, or as prior step for quantification of diseases like stenoses, aneurisms, or arteriosclerosis. To produce such descriptions two classes of approaches can be used: segmentation with a subsequent skeletonization or bottom up tube detection filters. As the top down segmentation problem is not a simple task which might require user interaction, bottom up tube detection filters are the state of the art methods used in several applications.

Most tube detection filters presented in the literature are based on the assumption that the tubular objects are bright structures in front of a darker homogeneous background; for example, [1,2,3,4,5,6]. The radius of these structures varies, but following the concepts of scale-space theory [7], the tubular structures form height-ridges when the scale is adapted accordingly to the size of the
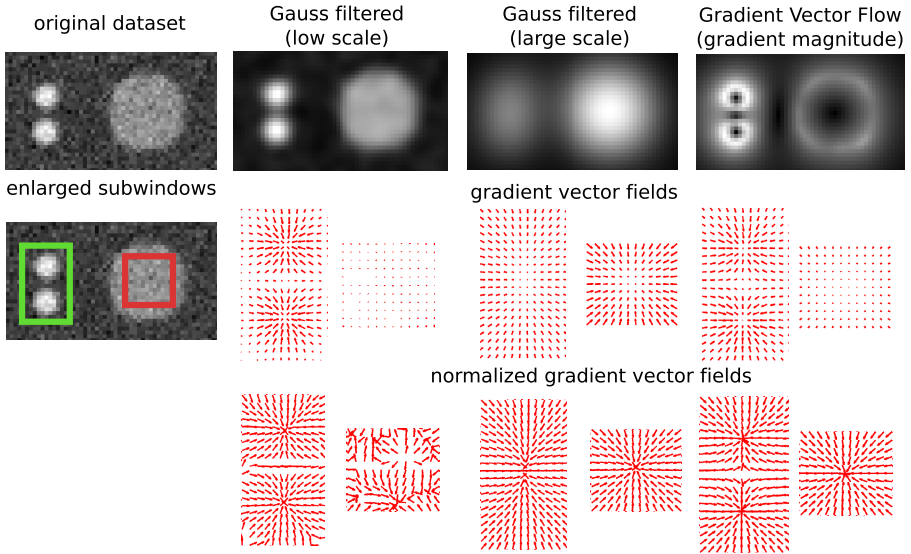

Fig. 1. 2D cross section (orthogonal to the tube's tangent direction) of 3D tubular structures and intermediate processing results of the multi-scale gradient vector compuation and the GVF

objects. Based on these assumptions, conventional tube detection filters try to identify the tubular objects at different scales and combine all responses into one multi-scale response. The response on a single scale is achieved by convolution of the initial image with a medialness function $K(\mathbf{x}, \sigma)$, where $\mathbf{x}$ is a point in 3D space and σ denotes the scale of the measurement. Typical medialness functions use the first order derivatives (gradient vectors), or second order derivatives (Hessian matrix), or a combination of both to identify the tubular objects at a specific scale; for example, [1,2,3,4,5,6]. They all have in common that a linear (Gaussian) scale space is used for computation of the spatial derivatives. This Gaussian smoothing is an isotropic diffusion that does not only result in suppression of noise but also in a blurring, which causes nearby features to diffuse into one another. This frequently leads to problems, e.g. that two tangenting tubes are detected as one single tube (see Fig. 1). For this reason, using the gradient vectors derived in a Gaussian scale space is generally not the appropriate choice for tube detection in medical images.

In this work, we address this problem and present a novel approach for detection of tubular objects. We propose to replace the isotropic diffusion of the image gradients by an anisotropic (edge preserving) diffusion process – namely the Gradient Vector Flow (GVF) [8] – and use the resulting vector field for detection of tubular objects. This avoids diffusion of nearby structures into one another and supersedes the computation at multiple scales. We discuss properties of the approach using synthetic datasets from public databases and demonstrate the applicability and advantage of our approach on clinical datasets.

The presented approach works in 2D as well as in 3D, for tubular structures brighter than the surrounding tissue or darker than the surrounding tissue. But for simplicity, in the remainder of the paper we will assume bright 3D tubular structures surrounded by darker tissue.

2   Methodology

As outlined in the introduction, tube detection filters utilize – directly or indirectly – the first order spatial derivatives to identify tubular objects. The reason is that tubular objects show characteristic gradient vector fields at their center-lines (see Fig. 1 bottom row) which can be used for classification. Therefore, the whole tube detection process can be split into two parts: deriving an appropriate gradient vector field V from the given image I and a subsequent classification based on this vector field. Both parts will be discussed separately in the next two paragraphs. A supporting example illustrating the basic idea on some tubular objects is shown in Fig. 1.

Generation of the gradient vector field: Conventional approaches for tube detection compute the gradient vector field at multiple scales. Given a specific scale σ, the gradient vector field V_σ is computed by convolution of the original image with a Gaussian filter kernel G_σ and computation of the local derivatives: $V_\sigma = \nabla(G_\sigma \star I) = G_\sigma \star \nabla I$. This can also be interpreted as a distribution of gradient information towards the center of the tubular object. When the scale is adapted appropriately to the size of the tube, the resulting vector field shows the typical characteristics of a tube at their centerlines (see Fig. 1 middle columns). However, when the scale gets larger, nearby objects diffuse into one another and may produce vector fields that can also be interpreted as tubular objects (see Fig. 1 middle right column). This behaviour is inherent in the linear scale space, as Gauss filtering is a non-feature-preserving diffusion process (isotropic diffusion).

To avoid diffusion of nearby objects into one another, it is necessary to replace the isotropic diffusion by a feature-preserving (edge-preserving) diffusion process. Anisotropic diffusion of the original image does not solve the problem, because for tube detection it is necessary to distribute gradient information from the boundary of the tubular object towards its center. The key is to perform a diffusion of the gradient information. A method that fulfills this requirement - edge-preserving diffusion of gradient information - is the GVF as presented by Xu and Prince [8]. The GVF is defined as the vector field $V(\mathbf{x})$ that minimizes:

$$E(V) = \iiint_\Omega \mu|\nabla V(\mathbf{x})|^2 + |\nabla I(\mathbf{x})|^2|V(\mathbf{x}) - \nabla I(\mathbf{x})|^2 d\mathbf{x}, \qquad (1)$$

where $\mathbf{x} = (x, y, z)$ and μ is a regularization parameter that has to be adapted according to the amount of noise present. The variational formulation of the GVF makes the result smooth where the initial vector magnitudes are small,

while keeping vectors with high magnitude nearly equal. In practice, the GVF preserves even weak structures while being robust to large amounts of noise [8].

For tubular objects applying the GVF results in the vector field shown on the very right column of Fig. 1. Compared to the vector fields derived from the Gaussian scale space, the GVF has two different properties: first, the problem of the linear scale space, diffusion of nearby structures into one another, is avoided. Second, at the centers of the tubular objects the GVF results in the same characteristic vector field as obtained with the multi-scale gradient computation when the scale is adapted appropriately to the tubes size. This allows detection of tubular objects (more precisely their centerlines) directly from the vector field produced by the GVF - without the need for a multi-scale analysis. Therefore, for the task of tube detection the GVF can be used as a replacement of the multi-scale gradient vector computation.

Classification based on the vector field: Having generated an appropriate vector field, the second step in tube detection is classification based on this vector field. As mentioned before, the GVF can - to some extent - be seen as a replacement for the multi-scale gradient vector computation, and the GVF's vector field can be combined with several tube detection filter approaches. We experimented with offset and central medialness functions published by other authors ([1,2,3]), achieving good results with all of them, but we decided to demonstrate the combination with Frangi's vesselness measure since it is simple and well known. Using the medialness functions of Pock et al. [3] or Krissian et al. [2] would also provide radius estimates for the tubes.

For a tubular object, the gradient vectors point all directly towards the centerline of the tube; the local vector field shows a large variance in two dimensions, and a low variance in the third dimension (see Fig. 1). One way to measure this variance is based on the Hessian matrix $H(\mathbf{x}) = \nabla V(\mathbf{x})$ and its eigenvalues $|\lambda_1| \leq |\lambda_2| \leq |\lambda_3|$. From these eigenvalues, it is possible to distinguish between plate-like, blob-like, and tubular structures (brighter or darker than the background) and noise. A frequently used measure to derive a tube-likeliness from the eigenvalues of the Hessian matrix is Frangi's vesselness measure [1]:

$$T = \begin{cases} 0 & \text{if } \lambda_2 > 0 \text{ or } \lambda_3 > 0 \\ \left(1 - exp\left(-\frac{R_A^2}{2\alpha^2}\right)\right)exp\left(-\frac{R_B^2}{2\beta^2}\right)\left(1 - exp\left(-\frac{S^2}{2c^2}\right)\right) & else \end{cases}$$

(2)

with $R_A = |\lambda_1|/\sqrt{|\lambda_2||\lambda_3|}$ indicating blob-like structures, $R_B = |\lambda_2|/|\lambda_3|$ to distinguish between plate-like and line-like structures, and $S = \sqrt{\lambda_1^2 + \lambda_2^2 + \lambda_3^2}$ for suppression of random noise effects. The parameters α, β, and c allow to control the sensitivity of the filter to the measures R_A, R_B, and S, respectively.

When combining Frangi's vesselness measure with the GVF, two adaptions are necessary. First, the third term of Frangi's vesselness measure that controls the noise-sensitivity becomes obsolete, as the noise-suppression is controlled by the regularization parameter μ of the GVF. Second, the magnitude of the GVF has to be normalized, $V^n(\mathbf{x}) = V(\mathbf{x})/|V(\mathbf{x})|$, because the original edge strength is not

of importance anymore (see Fig. 1 on the bottom right). Thus, the final response also becomes independent from the contrast of the tube and the centerlines of tubular objects can be extracted immediately by simple thresholding.

3 Evaluation and Results

In order to compare our approach to other methods and to demonstrate the difference between using a linear scale space and using the GVF for distribution of gradient information, we present results achieved with our approach and the results achieved with the method of Frangi et al. [1] and the method of Krissian et al. [2].

These two other approaches are multi-scale methods that operate in a Gaussian scale space. Frangi's method makes use of the eigenvalues of the Hessian matrix to derive a vesselness-measure as already presented in Sec. 2. Krissian's approach uses the Hessian matrix only to identify height ridges and to estimate the tubes orientation. In a second step, Krissian uses this information for selection of tube surface points and evaluates the gradient information at these points to derive his measure of medialness. For both approaches, the parameters suggested by the authors were used; with Frangi's approach it was necessary to adapt the noise-sensitivity parameter c according to the noise level.

With our approach, which also makes use of Frangi's vesselness measure, the following set of parameters was used, $\alpha = 0.5$, $\beta = 0.5$, $c = 100$, but instead of adapting c, the GVF's regularization parameter μ was adapted according to the noise level (default: $\mu = 0.1$). For low-noise datasets, the GVF was computed on the images directly without any preprocessing; for high-noise datasets, the images were slightly smoothed with a Gaussian filter with a standard deviation of one voxel, to account for image noise and partial voluming. If not mentioned explicitly, the images were not preprocessed. One may argue that this smoothing becomes a scale-space problem again; but, the slight smoothing only accounts for image noise and partial volume effects and does not take larger image areas into account. Therefore, the slight smoothing is only determined by the noise level and not the image content, and this is in contrast to Gauss filtering with a large scale filter kernel.

In order to visualize the datasets and to make the filter responses comparable, all images shown in the next sections were produced using maximum intensity projection for visualization; the gray value ranges of the datasets were normalized prior to visualization to show the full data range; exceptions are mentioned explicitly.

3.1 Synthetic Datasets

To demonstrate properties of the three methods under controlled reproducible conditions, we use synthetic datasets from two public databases and one synthetic dataset we created. These datasets allow us to study properties of the methods under varying noise conditions, contrast conditions, tube diameters and varying tube configurations as they occur in vascular systems. In these datasets,
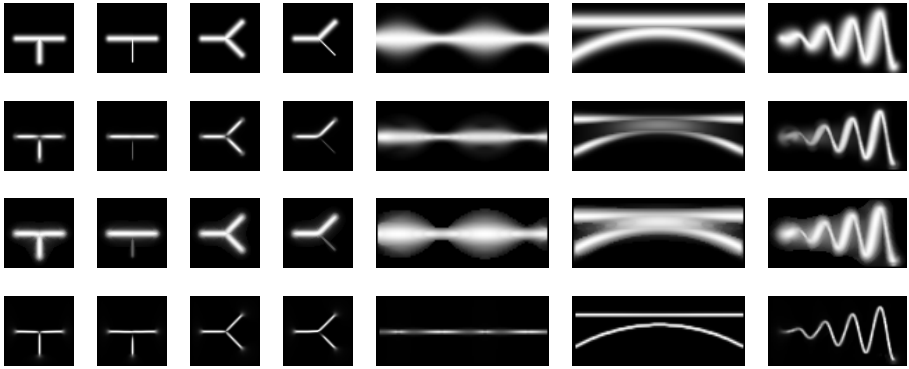
Fig. 2. Tubular objects in varying configurations and responses of the different methods. From top to bottom: original datasets, response of Frangi's method, Krissian's method, and our proposed method. From left to right: T-junction with constant diameter, T-junction with varying diameter, Y-junction with constant diameter, Y-junction with varying diameter, tube with varying diameter, tangenting tubes, helix.

the tubular objects show different kinds of edge-types as they appear in medical datasets: perfect step edges, slightly blurred step edges (due to partial voluming), and tubes with Gaussian cross-section profiles.

Varying tube configurations: The public database of Krissian and Farneback [2,9], see Fig. 2, shows standard situations of tubular objects, as they occur in vascular systems. For junctions of tubular objects with largely varying diameters, the response of our method falls off slightly, similar to the response of Frangi's method; but, as pointed out by Bennink et al. [4], this behaviour is common to most line filters and may be assumed as correct for pure lineness filters. With the example of the tube with the varying diameter, all methods allow for extraction of the correct centerline, but as the structure of this tube becomes more blob-like the response of Frangis's method and our proposed method falls off slightly; the response of Krissian's approach on the other hand is wider than the tubular object itself. The datasets with the tangenting tubes and the helix highlight the problem of the linear scale space analysis. Frangi's method, as well as Krissian's method, produce high responses outside the tubular objects, because on a larger scale these structures diffuse into one another; a separation is not possible anymore. In contrast, the response of our method is insensitive to influences outside the tubular objects and responds only at the correct centerline of the tubes.

Varying noise level: The dataset provided by Aylward et al. [10], see Fig. 3, contains a tortuous, branching, tubular object with vanishing radius. The contrast between the tubular object and the background ranges from 100 at the middle of the tube to 50 at the tube's edge. The datasets were corrupted with additive Gaussian noise with increasing standard deviations η of 10, 20, 40 and 80. "The $\eta = 20$ data is representative of the noise level in MR and CT data. The $\eta = 40$
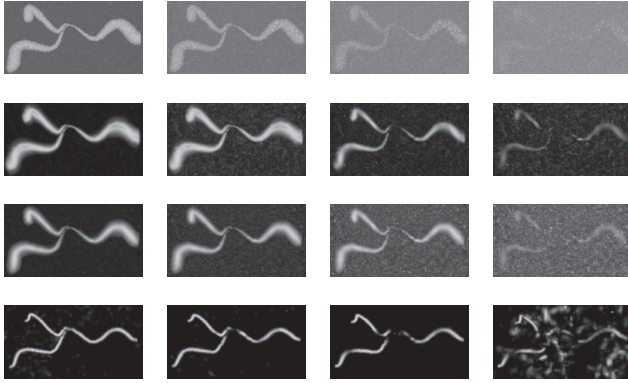
Fig. 3. Tubes with varying noise levels and responses of the different methods. From top to bottom: original datasets, response of Frangi's method, Krissian's method, and our proposed method. From left to right: increasing noise level using additive Gaussian noise with standard deviations η of 10, 20, 40, and 80.

data more closely resembles the noise magnitude of ultrasound data. [...] The $\eta = 80$ images are well beyond any worst case number [...] for any clinically acceptable MRA, CT, or ultrasound data."[10].

For Frangi's and our methods, the noise-sensitivity parameters, c and μ, respectively, had to be adapted. Krissian's method has no parameter that allows control of noise sensitivity. With our approach, on the $\eta = 10$ and $\eta = 20$ datasets the GVF was applied directly without any preprocessing; the $\eta = 40$ and $\eta = 80$ datasets were smoothed slightly using a Gaussian filter with a standard deviation of one voxel.

The results show that our approach produces clean responses at the centers of the tubular objects even under high (clinically acceptable) noise levels ($\eta = 10$, 20, and 40). On the $\eta = 80$ dataset, the results of all methods are not satisfying.

Varying contrast and diameter: The dataset shown in Fig. 4 on the very left shows tubular structures with different radii. The background intensity of the image was steadily increased, thus resulting in a decreased contrast between the tube and the background. The responses of the method of Frangi and Krissian both depend on the contrast between the tube and the background. Thus, their response decreases with decreasing contrast. In comparison, the response of our method is independent of the tubes size and contrast.

3.2   Clinical Datasets

In this section, we apply the three methods to two medical volume datasets and verify the results obtained on the synthetic datasets on clinical datasets.

CT angiography: In the top row of Fig. 5, a CT angiography image and enlarged subregions with challenging situations are shown. The main problems for tube
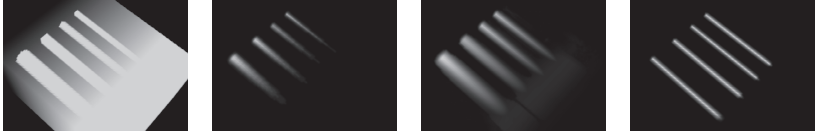
Fig. 4. Tubes with varying diameter and contrast and the responses of the different methods. From left to right: original dataset, response of Frangi's method, Krissian's method, and our proposed method.

detection filters with this kind of dataset are the detection of very thin low contrast vessels, diffuse edges, and closely adjacent vessels. Frangi's and Krissian's methods were specifically designed for angiography images. With our approach, the GVF was applied directly to the dataset, without any preprocessing, as the conditions are comparable to the synthetic datasets from Krissian's database (see Sec. 3.1).

The overview image of the whole dataset (leftmost column) shows that our approach works similarly well for wide tubes with bar-like cross-section profiles and
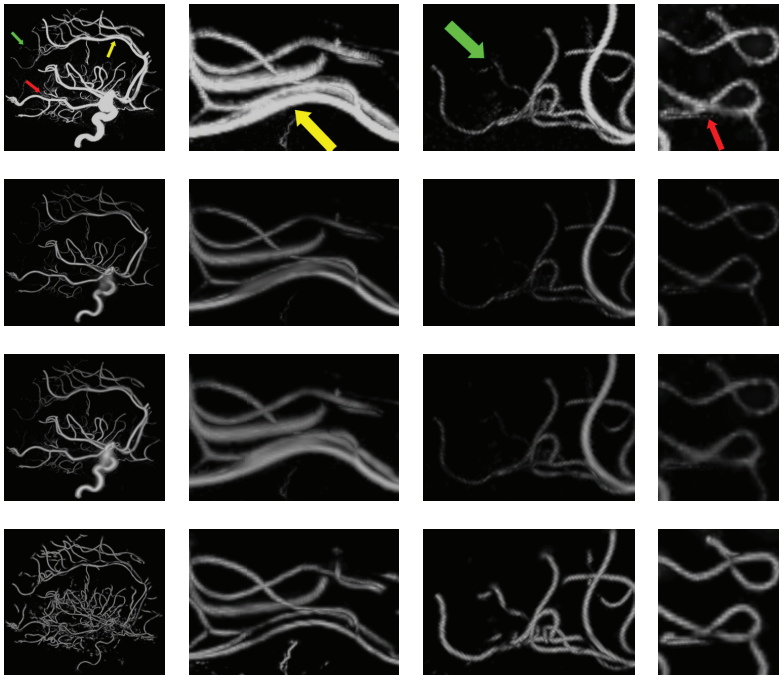

Fig. 5. CT angiography image and responses of the different methods. From top to bottom: original dataset, response of Frangi's method, Krissian's method, and our proposed method. From left to right: overview of the whole dataset, closely tangenting vessels (yellow arrow), thin vessels (green arrow), overlapping vessels (red arrow).

for very thin tubular objects with Gaussian cross-section profiles. The magnified subregion showing the tangenting tubes (middle left column), verifies the results of the synthetic datasets; Frangi's and Krissian's multi-scale approaches diffuse the closely adjacent structures into one another, making an extraction of height ridges as suggested by Krissian et al. [2] for centerline extraction impossible; our approach allows a clear separation of both. The magnified subregion shows some very thin low contrast vessels (middle right column). As the responses of Frangi's and Krissian's methods decrease with decreasing contrast (see Sec. 3.1) the response to low contrast vessels also decreases. This makes a separation from the background difficult (e.g. based a single threshold as suggested by Krissian et al. [2]); our approach is insensitive to changing contrast situations and finding a single threshold for extraction of the centerlines is an easy task. The magnified subregion on the very right column shows another example of very thin tubular structures; the vessels overlap completely in the image because of partial voluming. None of the three methods is able to separate them because they do not take sub-pixels into account.

CT of the aorta: To demonstrate the performance of the different methods in a more complex environment and with a higher noise level, the methods have been applied to a CT dataset of the abdomen showing the aorta, see Fig. 6. With our approach, the dataset was preprocessed using a Gaussian filter with a standard deviation of one voxel (intra-slice resolution). This example reveals the drawback of the linear scale space very clearly: the close proximity of spine and aorta disturbs the detection of the aorta when applying Franig's or Krissian's method. Both produce undesired responses to several structures in the image. One may think of the whole spine as a tubular object at a large scale, but this disturbs the detection
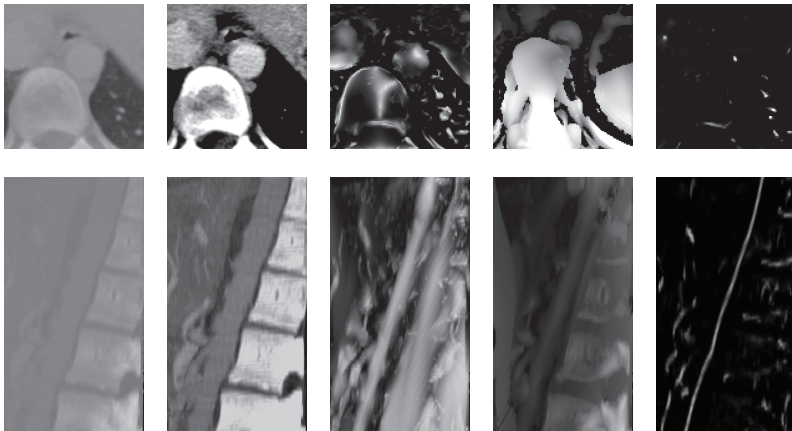

Fig. 6. CT of the abdomen showing the aorta in proximity to the spine. Top row: axial slice; Bottom row: maximum intensity projection. From left to right: original dataset showing the full data range, original dataset with adapted gray value range, response of Frangi's method (adapted gray value range), Krissian's method (adapted gray value range), and our proposed method.

of smaller vessels in its close proximity. With our approach, the detection of the aorta is not influenced at all by any surrounding object.

4   Conclusion

In this work, we addressed a common problem of most tube detection filters that is related to the multi-scale gradient vector computation in the conventionally used Gaussian scale space: diffusion of nearby structures into one another that may result in additionally detected tubular structures. We showed that this problem can be avoided by using the GVF as a replacement for the multi-scale gradient vector computation. In combination with Frangi's vesselness measure, the resulting approach allows detection of centerlines of tubular objects, independent of the tubes size and contrast.

References

1. Frangi, A.F., Niessen, W.J., Vincken, K.L., Viergever, M.A.: Multiscale vessel enhancement filtering. In: Wells, W.M., Colchester, A.C.F., Delp, S.L. (eds.) MICCAI 1998. LNCS, vol. 1496, pp. 130–137. Springer, Heidelberg (1998)
2. Krissian, K., Malandain, G., Ayache, N., Vaillant, R., Trousset, Y.: Model-based detection of tubular structures in 3D images. Computer Vision and Image Understanding 80(2), 130–171 (2000)
3. Pock, T., Beichel, R., Bischof, H.: A novel robust tube detection filter for 3d centerline extraction. In: Kalviainen, H., Parkkinen, J., Kaarna, A. (eds.) SCIA 2005. LNCS, vol. 3540. Springer, Heidelberg (2005)
4. Bennink, H.E., van Assen, H.C., ter Wee, R., Spaan, J.A.E., ter Haar Romeny, B.M.: A novel 3D multi-scale lineness filter for vessel detection. In: Ayache, N., Ourselin, S., Maeder, A. (eds.) MICCAI 2007, Part II. LNCS, vol. 4792, pp. 436–443. Springer, Heidelberg (2007)
5. Lorenz, C., Carlsen, I.C., Buzug, T.M., Fassnacht, C., Weese, J.: Multi-scale line segmentation with automatic estimation of width, contrast and tangential direction in 2d and 3d medical images. In: Troccaz, J., Mösges, R., Grimson, W.E.L. (eds.) CVRMed-MRCAS 1997, CVRMed 1997, and MRCAS 1997. LNCS, vol. 1205, pp. 233–242. Springer, Heidelberg (1997)
6. Sato, Y., Nakajima, S., Shiraga, N., Atsumi, H., Yoshida, S., Koller, T., Gerig, G., Kikinis, R.: Three-dimensional multi-scale line filter for segmentation and visualization of curvilinear structures in medical images. MIA 2(2), 143–168 (1998)
7. Lindeberg, T.: Edge detection and ridge detection with automatic scale selection. In: CVPR 1996, Washington, DC, USA, p. 465. IEEE Computer Society, Los Alamitos (1996)
8. Xu, C., Prince, J.L.: Snakes, shapes, and gradient vector flow. IEEE Transactions on Image Processing 7(3), 359–369 (1998)
9. Krissian, K., Farneback, G.: Building reliable clients and servers. In: Leondes, C.T. (ed.) Medical Imaging Systems Technology: Methods in Cardiovascular and Brain Systems, World Scientific Publishing Co., Singapore (2005)
10. Aylward, S., Bullit, E.: Initialization, noise, singularities, and scale in height ridge traversal for tubular object centerline extraction. IEEE Transactions on Medical Imaging 21(2), 61–75 (2002)